Mesoporous Silica-Coated Gold Nanorods as a Light-Mediated Multifunctional Theranostic Platform for Cancer Treatment

Zhenjiang Zhang, Liming Wang, Jing Wang, Xiumei Jiang, Xiaohui Li, Zhijian Hu, Yinglu Ji, Xiaochun Wu, and Chunying Chen**

The unique physicochemical properties of nanomaterials have offered an opportunity to integrate different theranostic modalities into a single nanoplatform for combined cancer treatments with real-time diagnosis.[1] In particular, gold nanostructures (AuNSs), such as gold nanorods (AuNRs) and nanoshells are being actively studied as a promising and versatile platform for cancer theragnosis.[2] Due to tunable localized surface plasmon resonance (LSPR), AuNSs are not only attractive probes for cancer cell imaging,[1b,2c,3] but they can also become highly localized heat sources when irradiated with a laser through the photothermal effect.[2c] The generated heat can be used to provide hyperthermal cancer therapy[2b,c,3a,4] and/or to trigger drug release for chemotherapeutics when AuNSs serve as an anticancer-drug carrier.[5] Thus, there is a possibility to realize imaging, chemotherapeutics, and hyperthermia within a single AuNSs platform for cancer treatments with a potential to establish new therapeutic modes, such as image-guided drug delivery and hyperthermia, and combination therapy. Development of such multifunctional theranostic systems with individual functions acting in a coordinated way is critical to optimize therapeutic efficacy and safety of therapeutic regimes, and could provide more opportunities for on-demand therapy and pave the road toward personalized medicine.

AuNRs with an LSPR maximum between 650 and 950 nm are considered to have great potential for various light-based imaging and therapeutic techniques. However, as a theranostic platform, AuNRs bear two disadvantages: a relatively low specific surface area limits the loading amount of drugs, and due to the often-observed clustering and aggregating of the AuNRs within cells, the desirable NIR window is shifted to the visible spectral region, which thus loses the advantage of deep-tissue penetration. In order to overcome these two drawbacks, we herein report our efforts in developing mesoporous silica-coated gold nanorods ($Au@SiO_2$) as a novel cancer theranostic platform. The large specific surface area of mesoporous silica guarantees a high drug payload. With the protection and/or shielding of silica shell (~30 nm), the LSPR maximum is reserved for the optimized light-transparent window. To demonstrate the multiple functionalities of the new platform, a well-known chemotherapy drug, doxorubicin hydrochloride (DOX), was employed as a model drug. The theranostic principle based on the unique properties of the $Au@SiO_2$ is illustrated in **Figure 1**A. One imaging modality of the AuNRs, two-photon imaging (TPI), is employed to visualize the intracellular colocalization of $Au@SiO_2$ with DOX and some cellular compartments. NIR laser irradiation at a low intensity is used to enhance drug release from DOX-loaded $Au@SiO_2$ ($Au@SiO_2$–DOX) for chemotherapy, while at higher irradiation intensity it also triggers hyperthermia of the AuNRs. $Au@SiO_2$ can thus provide two therapeutic modes for cancer treatments. Our in-vitro results establish $Au@SiO_2$ as a promising and versatile theranostic platform and suggest its potential in-vivo applications.

$Au@SiO_2$ were fabricated according to a reported protocol with some modifications (see the Supporting information (SI)).[6] In the silica-coating process, cetyltrimethylammonium bromide (CTAB) formed a bilayer around the AuNRs and served as an organic template for the formation of the mesoporous silica layer. From transmission electron microscope (TEM) images of the synthesized $Au@SiO_2$, the amorphous silica shell is estimated to have a homogeneous thickness of ~30 nm and is composed of disordered mesopores of ~5 nm in diameter (Figure 1B,C), offering an opportunity for $Au@SiO_2$ to be used as a general drug carrier. The as-prepared AuNRs have a longitudinal SPR peak at 760 nm (Figure 1D). After silica-shell coating, it exhibits a small red-shift (~20 nm), consistent with the corresponding theoretical simulation (SI, Figure S1A, finite difference time domain, FDTD). Due to the large distance between the AuNRs in $Au@SiO_2$, clustering and aggregating will not influence the location of the longitudinal SPR band in the NIR window (SI, Figure S1), thus permitting photons to penetrate biological tissues with relatively high transmissivity, indicating the high potential for $Au@SiO_2$ to be applied theranostically in epithelial tissues.[5d,7] In contrast, the AuNR dimer without a silica shell shifts its longitudinal SPR maximum to

Dr. Z. Zhang, Dr. L. Wang, J. Wang, X. Jiang, Dr. X. Li, Prof. C. Chen
CAS Key Laboratory for Biomedical
Effects of Nanomaterials and Nanosafety
National Center for Nanoscience and Technology
No.11 Zhongguancun Beiyitiao
Beijing 100190, China
E-mail: chenchy@nanoctr.cn
Dr. Z. Hu, Y. Ji, Prof. X. Wu
CAS Key Laboratory of Standardization
and Measurement for Nanotechnology
National Center for Nanoscience and Technology
No.11 Zhongguancun Beiyitiao
Beijing 100190, China
E-mail: wuxc@nanoctr.cn
Dr. L. Wang
Institute of High Energy Physics
Chinese Academy of Sciences
No.19B Yuquanlu, Beijing 100049, China

DOI: 10.1002/adma.201104714

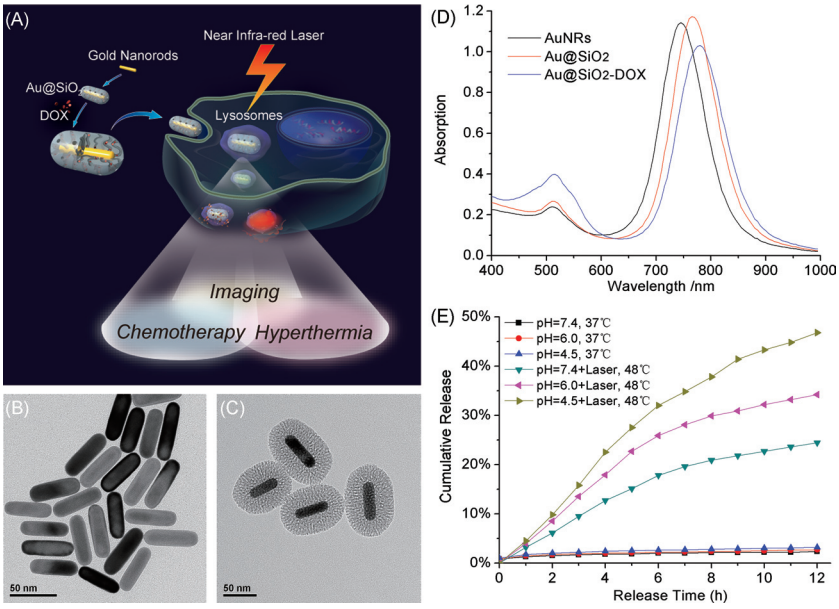

Figure 1. A) Schematic illustration of mesoporous silica-coated gold nanorods (Au@SiO_2) as a novel multifunctional theranostic platform for cancer treatment. TEM images of B) AuNRs and C) Au@SiO_2, D) extinction spectra of AuNRs, Au@SiO_2, and Au@SiO_2–DOX, and E) DOX release profiles from Au@SiO_2–DOX with and without NIR laser irradiation at different pHs.

shorter wavelengths, thus potentially leading to a loss of the optimized laser wavelength (SI, Figure S1). Considering the complicated aggregation behaviors of AuNRs within different cells, it becomes quite difficult to predict the optimized laser wavelength for real systems using AuNRs without silica shells. In addition, the mesoporous structure of the shell allows exposure of the AuNR core to the surrounding medium, thus enabling a sensitive response of the longitudinal SPR mode to refractive index changes caused by adsorbed molecules:[8] a further red-shift accompanying slight damping of the band is observed upon DOX adsorption (Figure 1D).

DOX was loaded into the mesopores of Au@SiO_2 at pH 7.4 through electrostatic interactions and formed an Au@SiO_2–DOX complex. By varying the concentrations of DOX and Au@SiO_2, the loading content reached up to 14.5% (SI, Table S1). The weight ratio of SiO_2 and gold in Au@SiO_2 was estimated to be ~0.67 by TEM/energy dispersive spectroscopy (EDS) analysis (SI, Figure S2C). Therefore, if only the weight of the silica layer is counted, the loading content could reach 29.7% (w/w), comparable to that of those typical mesoporous silica nanoparticles (MSNs).[9]

The in-vitro drug release behaviors of Au@SiO_2–DOX were studied in buffers at different pHs at 37° (Figure 1E). In the absence of laser irradiation, the cumulative release amount of DOX is quite small and the difference in release amounts between different pHs is not significant. This slow DOX release behavior is similar to those typical MSNs encapsulated with DOX, suggesting strong electrostatic interactions between DOX and dissociated silanols.[9a,b] To achieve a faster DOX release, we used a 250 mW NIR laser (wavelength 780 nm) to irradiate and heat the Au@SiO_2–DOX solution up to 48 °C (SI, Figure S3). Under laser irradiation, the drug release rate becomes much faster for any pH, because the laser-converted heat dissociates the strong interactions between DOX and silica and thus more DOX molecules are released (Figure 1E). Also observed is a pH-dependent release behavior with more DOX released at lower pHs.[9b] This is because more surface silanols are protonated with the decrease of pH, also leading to a decrease in the electrostatic interaction and dissociation of DOX from the silica surface. It is noteworthy that Au@SiO_2–DOX has a sustained-release property which is useful for those clinical cases that require a high dose followed by a constant release of smaller dosage.[10] Since light can be manipulated very precisely, the Au@SiO_2 provides an ideal platform to deliver anticancer agents such as DOX in a light-activation mechanism with exact control of the area, time, and dosage.[7b]

One desired property of a drug carrier is that it can increase drug uptake and accumulation.[11] Herein, we compared the internalization of free DOX and Au@SiO_2–DOX by A549 cells using flow cytometry to detect the fluorescence signal of intracellular DOX. Our results show that about 5–10 times more DOX could be internalized when they were loaded in Au@SiO_2 (**Figure 2**A). The positive zeta potential of Au@SiO_2–DOX (SI, Table S2) might account for the increased cell uptake, as cell membranes are negatively charged, thus showing stronger interactions with positively charged nanoparticles.[2c,12] By using a two-photon confocal microscope, we further visualized the colocalization of DOX, lysosomes, and mitochondria with Au@SiO_2–DOX. Most nanoparticles were found to remain in endosomes/lysosomes and only a small amount entered mitochondria (Figure 2B,C, and SI, S4). These results also demonstrate that AuNRs show a pronounced ability as TPI contrast agents when in the form Au@SiO_2–DOX, which may later offer an opportunity for image-guided chemotherapy and/or hyperthermia.[1a,13] The cytotoxicity of Au@SiO_2, free DOX, and Au@SiO_2–DOX to A549 cells was evaluated by a CCK-8 assay. Au@SiO_2 showed negligible toxicity (Figure 2F) while both free DOX and Au@SiO_2–DOX caused time- and dose-dependent cytotoxicity (Figure 2D,E). Au@SiO_2–DOX was obviously less toxic than free DOX, which suggested that only a limited portion of DOX was released into cells in the absence of laser irradiation.

Since Au@SiO_2–DOX complexes accumulate in intracellular vesicles like lysosomes with a high local concentration (Figure 2B), two anticancer therapeutic modes, DOX release for chemotherapy and hyperthermia, are both possible if the cells are irradiated with a laser. To investigate the hyperthermic potential of Au@SiO_2–DOX, two groups of human lung cancer cells (A549) with Au@SiO_2–DOX internalized were irradiated with, respectively, 24 and 48 W cm^{-2} laser light, and the lysosomal membrane permeation (LMP) was analyzed using acridine orange (AO) staining to determine whether LMP can be changed by laser-converted heat. We observed a strong disruption in the lysosomal membrane immediately after 3 min of the 48 W cm^{-2} laser irradiation. Increased blebbings around

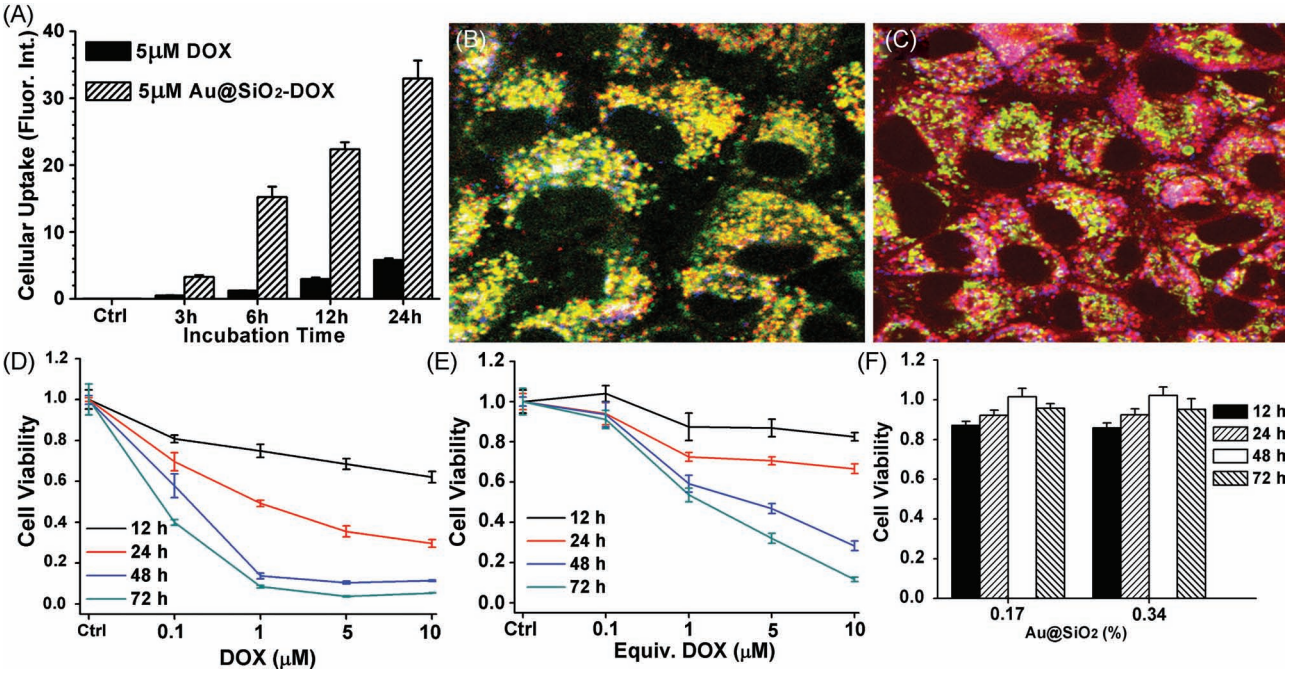

Figure 2. A) Cellular uptake of DOX and Au@SiO_2–DOX quantified by flow cytometry. B,C) Intracellular localization of DOX (red) and Au@SiO_2 (blue) with organelle-specific probes including Lyso-Tracker (green) and Mito-Tracker (green) using two-photon confocal microscope. The process of translocation of intracellular DOX was assessed using a fluorescence microscope. Time- and dose-dependent effects of D) DOX, E) Au@SiO_2–DOX, and F) Au@SiO_2 on the viability of A549 cells (the equivalent DOX concentrations of 0.17% and 0.34% Au@SiO_2 are 5 μM and 10 μM, respectively.

the cell membrane, which will inevitably lead to acute (fast) cell death, appeared after the lysosomal membrane was destroyed (**Figure 3**C). For Au@SiO_2–DOX-untreated cells, irradiation with the same laser caused negligible effect on LMP (Figure 3A). In the case of 24 W cm^{-2} laser irradiation, A549 cells maintained an unchanged LMP and intact cell membrane (Figure 3B). These results are consistent with previous reports that there existed a threshold laser power for tumoricidal efficacy of AuNR-mediated hyperthermia.[14] In this study, the threshold is much higher than the reported ~10 W cm^{-2}, which might be due to the difference in the internalized quantity of AuNRs. The silica shell around the AuNRs may have also prevented, to some extent, the laser-converted heat from causing acute damage to the lysosomal membrane.

The chemotherapeutic potential of Au@SiO_2–DOX was explored using a lower power density laser of 20 W cm^{-2} to avoid killing A549 cells directly through the hyperthermic effect. Cell viability was analyzed by Live–Dead assay (**Figure 4**B) and CCK-8 assay (Figure 4A). For both untreated and Au@SiO_2-treated cells, 3 min irradiation by the NIR laser neither increased cell death nor decreased cell viability in the following 24 h. In the case of Au@SiO_2–DOX-incubated cells, no acute cell death or loss of cell viability was observed immediately after 3 min irradiation. However, a slight increase in cell death occurred at 12 h after irradiation and a significant increase in cell death and an obvious loss of cell viability were observed at 24 h after irradiation. Based on the fact that the 24 W cm^{-2} laser irradiation didn't cause any acute damage to Au@SiO_2–DOX-incubated cells and no loss of cell viability happened in 24 h in blank Au@SiO_2-incubated cells with 20 W cm^{-2} laser irradiation, we attribute the above curative results to the chemotherapeutic ability of Au@SiO_2–DOX, that is, the NIR laser triggered DOX release within cells. A reasonable explanation of the delayed effects is that a certain period of time may be needed for the released DOX in lysosomes to translocate to its target DNA within nuclei. We then prolonged the irradiation times from 3 to 4 and 8 min, but found the cell viability at 24 h only decreased slightly (Figure 4B). This further supports that it is the chemotherapy, not the hyperthermia, that produced the curative effect of the treatment because the hyperthermic results should be reasonably related with the duration of laser irradiation.

The Au@SiO_2–DOX with laser irradiation thus provides two therapeutic modes: chemotherapy through low-power-density laser-triggered DOX release, and hyperthermia therapy under high-power-density laser irradiation. Both modes are inherently localized, since only cancerous tissue need be irradiated by the laser. Compared to traditional systematic cancer treatments, localized therapies are able to enhance tumoricidal efficacy and decrease side effects.[15] Targeting ligands, such as arginine–glycine–aspartic acid (RGD) peptides or transferrin might be conjugated to the surface of Au@SiO_2 to explore its localized therapeutic potential in vivo.[16] In addition, after intravenous injection, the positive nanoparticles would first interact with blood proteins. In turn, the resulting protein-coated Au@SiO_2–DOX may help their transportation and behavior in vivo. Combination of the two therapeutic modes is helpful to overcome some serious challenges faced by monotherapies. For instance, chemotherapy resistance occurs in half of all patients and may

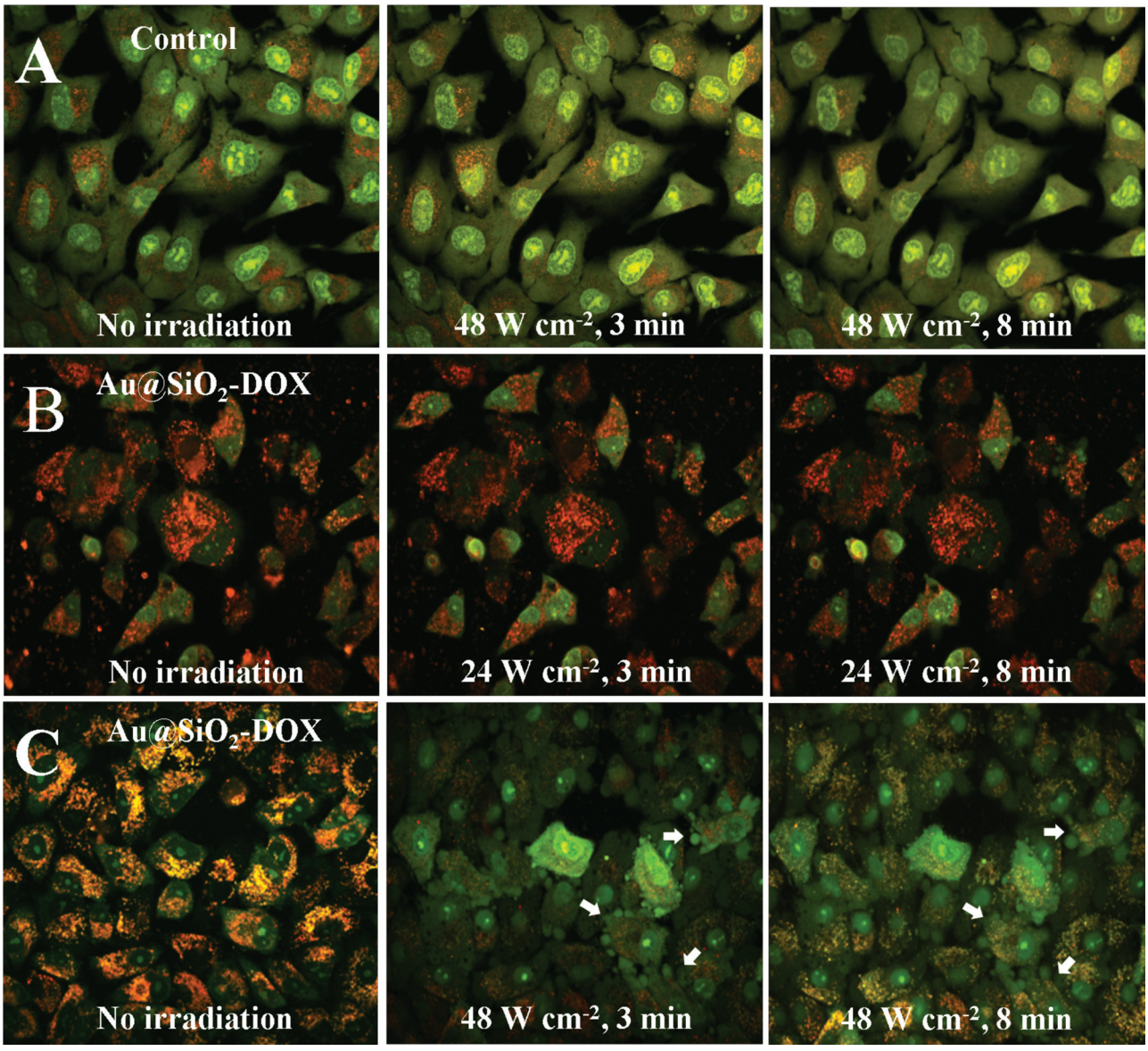

Figure 3. The effects of NIR-laser irradiation on lysosomal membrane integrity determined by acridine orange (AO) staining. Au@SiO_2–DOX-untreated A549 cells are used as controls and irradiated by a NIR laser (790 nm, 48 W cm^{-2}) (A). Au@SiO_2–DOX (containing 5 μM DOX)-treated cells are irradiated by laser (790 nm) with two different power densities, 24 W cm^{-2} (B) and 48 W cm^{-2} (C), for 0, 3, and 8 min.

lead to treatment failure,[17] while hyperthermal therapy usually requires sophisticated temperature control to achieve the desired level of efficacy and avoid damages to noncancerous tissue.[1c] The combination of chemotherapy and hyperthermia in a single platform can, therefore, extend their applications and might be employed synergistically to treat high-risk tumors with a goal of complete tumor eradication. One additional advantage of Au@SiO_2–DOX mediated combination of chemotherapy and hyperthermia is that the therapeutic mode can be switched freely by changing laser power density.

In this work, Au@SiO_2 as a multifunctional theranostic platform was demonstrated in vitro. The inner AuNR core functions both as TPI imaging agent and hyperthermia agent. The outer mesoporous SiO_2 shell exhibits the potential for allowing a high drug payload, thus posing itself as an effective drug carrier. Additionally, the protection of the silica shell guarantees the utilization of the NIR-transparent window provided by the AuNR core in complex biological environments. More interestingly, the incorporation of the two nanomaterials created a new functionality: NIR laser-controlled drug release. For the goal of on-demand therapy and personalized medicine, the therapeutic modes of Au@SiO_2–DOX, either chemotherapy or hyperthermia, can be manipulated simply by changing laser power density. Such a versatile theranostic system as Au@SiO_2–DOX is expected to have wide biomedical application and may be particularly useful for cancer therapy.

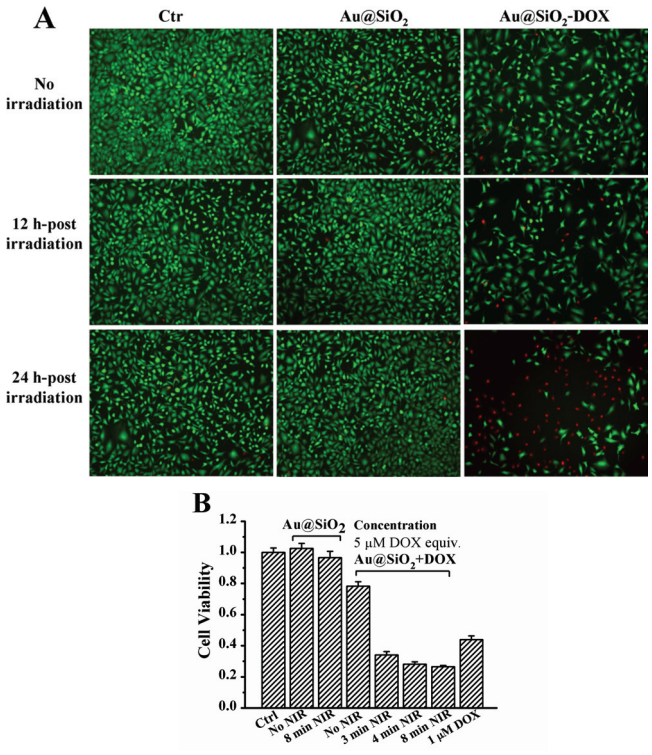

Figure 4. NIR light-triggered DOX release within cells for chemotherapy and its influence on cell viability. A) Live–Dead staining of A549 cells 12 and 24 h post-irradiation. A549 cells are treated with $Au@SiO_2$ or $Au@SiO_2$–DOX for 12 h and then radiated for 3 min using a NIR laser with power density of 20 W cm^{-2}. B) Differences in viability of A549 cells irradiated by NIR laser for 8 min ($Au@SiO_2$) and for 3, 4, and 8 min ($Au@SiO_2$–DOX), determined by CCK-8 assay.

Experimental Section

Detailed experimental materials and methods can be found in the Supporting Information.

Supporting Information

Supporting Information is available from the Wiley Online Library or from the author. It includes methods for the synthesis and characterization of $Au@SiO_2$, drug loading and release, cell uptake, cell viability assays, intracellular localization, and laser irradiation experiments.

Acknowledgements

Z. Zhang, L. Wang, and J. Wang contributed equally to this work. This work was supported financially by the National Basic Research Program of China (2010CB93404, 2011CB933401 and 2012CB93401), the National Natural Science Foundation of China (31070854), the Major National S&T Program, and the Knowledge Innovation Program of the Chinese Academy of Sciences.

Received: December 10, 2011
Revised: December 26, 2011
Published online: February 9, 2012

[1] a) P. Rai, S. Mallidi, X. Zheng, R. Rahmanzadeh, Y. Mir, S. Elrington, A. Khurshid, T. Hasan, *Adv. Drug Deliv. Rev.* **2010**, *62*, 1094; b) J. Xie, S. Lee, X. Chen, *Adv. Drug Deliv. Rev.* **2010**, *62*, 1064; c) J. Yang, J. Lee, J. Kang, S. J. Oh, H.-J. Ko, J.-H. Son, K. Lee, J.-S. Suh, Y.-M. Huh, S. Haam, *Adv. Mater.* **2009**, *21*, 4339; d) R. Guo, L. Zhang, H. Qian, R. Li, X. Jiang, B. Liu, *Langmuir* **2010**, *26*, 5428; e) K. Riehemann, S. W. Schneider, T. A. Luger, B. Godin, M. Ferrari, H. Fuchs, *Angew. Chem. Int. Ed.* **2009**, *48*, 872; f) J. Xie, G. Liu, H. S. Eden, H. Ai, X. Chen, *Acc. Chem. Res.* **2011**, *44*, 883.

[2] a) L. Tong, Q. S. Wei, A. Wei, J. X. Cheng, *Photochem. Photobiol.* **2009**, *85*, 21; b) A. M. Alkilany, L. B. Thompson, S. P. Boulos, P. N. Sisco, C. J. Murphy, *Adv. Drug Deliv. Rev.* **2011**, DOI: 10.1016/j.addr.2011.03.005; c) C. M. Cobley, J. Chen, E. C. Cho, L. V. Wang, Y. Xia, *Chem. Soc. Rev.* **2011**, *40*, 44.

[3] a) H. Ke, J. Wang, Z. Dai, Y. Jin, E. Qu, Z. Xing, C. Guo, X. Yue, J. Liu, *Angew. Chem. Int. Ed.* **2011**, *50*, 3017; b) C. Ungureanu, R. Kroes, W. Petersen, T. A. Groothuis, F. Ungureanu, H. Janssen, F. W. van Leeuwen, R. P. Kooyman, S. Manohar, T. G. van Leeuwen, *Nano Lett.* **2011**, *11*, 1887; c) W. Ni, Z. Yang, H. Chen, L. Li, J. Wang, *J. Am. Chem. Soc.* **2008**, *130*, 6692.

[4] a) P. Diagaradjane, A. Shetty, J. C. Wang, A. M. Elliott, J. Schwartz, S. Shentu, H. C. Park, A. Deorukhkar, R. J. Stafford, S. H. Cho, J. W. Tunnell, J. D. Hazle, S. Krishnan, *Nano Lett.* **2008**, *8*, 1492; b) H. Shen, J. You, G. Zhang, A. Ziemys, Q. Li, L. Bai, X. Deng, D. R. Erm, X. Liu, C. Li, M. Ferrari, *Adv. Healt. Mater.* **2011**, DOI: 10.1002/adhm.201100005.

[5] a) Y. Jin, X. Gao, *J. Am. Chem. Soc.* **2009**, *131*, 17774; b) G. D. Moon, S.-W. Choi, X. Cai, W. Li, E. C. Cho, U. Jeong, L. V. Wang, Y. Xia, *J. Am. Chem. Soc.* **2011**, *133*, 4762; c) H. Takahashi, Y. Niidome, S. Yamada, *Chem. Commun.* **2005**, 2247; d) C. C. Chen, Y. P. Lin, C. W. Wang, H. C. Tzeng, C. H. Wu, Y. C. Chen, C. P. Chen, L. C. Chen, Y. C. Wu, *J. Am. Chem. Soc.* **2006**, *128*, 3709; e) J. You, R. Shao, X. Wei, S. Gupta, C. Li, *Small* **2010**, *6*, 1022; f) S. Yamashita, H. Fukushima, Y. Akiyama, Y. Niidome, T. Mori, Y. Katayama, T. Niidome, *Biorg. Med. Chem.* **2011**, *19*, 2130.

[6] I. Gorelikov, N. Matsuura, *Nano Lett.* **2008**, *8*, 369.

[7] a) T. Niidome, A. Shiotani, Y. Akiyama, A. Ohga, K. Nose, D. Pissuwan, Y. Niidome, *Yakugaku Zasshi* **2010**, *130*, 1671; b) G. Mayer, A. Heckel, *Angew. Chem. Int. Ed.* **2006**, *45*, 4900.

[8] a) C. Wu, Q.-H. Xu, *Langmuir* **2009**, *25*, 9441; b) G. Wang, Z. Chen, L. Chen, *Nanoscale* **2011**, *3*, 1756.

[9] a) A. Bernardos, L. Mondragon, E. Aznar, M. D. Marcos, R. Martinez-Manez, F. Sancenon, J. Soto, J. M. Barat, E. Perez-Paya, C. Guillem, P. Amoros, *ACS Nano* **2010**, *4*, 6353; b) L. Yuan, Q. Q. Tang, D. Yang, J. Z. Zhang, F. Y. Zhang, J. H. Hu, *J. Phys. Chem. C* **2011**, *115*, 9926; c) L. S. Wang, L. C. Wu, S. Y. Lu, L. L. Chang, I. T. Teng, C. M. Yang, J. A. Ho, *ACS Nano* **2010**, *4*, 4371.

[10] T. T. Wang, F. Chai, C. G. Wang, L. Li, H. Y. Liu, L. Y. Zhang, Z. M. Su, Y. Liao, *J. Coll. Interf. Sci.* **2011**, *358*, 109.

[11] a) L. Wang, Y. F. Li, L. Zhou, Y. Liu, L. Meng, K. Zhang, X. Wu, L. Zhang, B. Li, C. Chen, *Anal. Bioanal. Chem.* **2010**, *396*, 1105; b) X. Jiang, L. Wang, C. Chen, *J. Chin. Chem. Soc.* **2011**, *58*, 273; c) Y. Gao, C. Chen, Z. Chai, *J. Anal. Atom. Spectrom.* **2007**, *22*, 856.

[12] a) Y. Qiu, Y. Liu, L. M. Wang, L. G. Xu, R. Bai, Y. L. Ji, X. C. Wu, Y. L. Zhao, Y. F. Li, C. Y. Chen, *Biomaterials* **2010**, *31*, 7606; b) L. Wang, Y. Liu, W. Li, X. Jiang, Y. Ji, X. Wu, L. Xu, Y. Qiu, K. Zhao, T. Wei, Y. Li, Y. Zhao, C. Chen, *Nano Lett.* **2011**, *11*, 772; c) J. M. Rosenholm, C. Sahlgren, M. Linden, *Nanoscale* **2010**, *2*, 1870.

[13] Y. S. Chen, W. Frey, S. Kim, K. Homan, P. Kruizinga, K. Sokolov, S. Emelianov, *Opt. Exp.* **2010**, *18*, 8867.

[14] a) L. Tong, Q. Wei, A. Wei, J.-X. Cheng, *Photochem. Photobiol.* **2009**, *85*, 21; b) L. Tong, J.-X. Cheng, *Nanomedicine* **2009**, *4*, 265; c) L. Tong, Y. Zhao, T. B. Huff, M. N. Hansen, A. Wei, J. X. Cheng, *Adv. Mater.* **2007**, *19*, 3136.
[15] X. Li, C. Zhang, L. Le Guyader, C. Chen, *Sci. Chin. Chem.* **2010**, *53*, 2241.
[16] a) K. N. Sugahara, T. Teesalu, P. P. Karmali, V. R. Kotamraju, L. Agemy, D. R. Greenwald, E. Ruoslahti, *Science* **2010**, *328*, 1031; b) Z. M. Li, P. Huang, X. J. Zhang, J. Lin, S. Yang, B. Liu, F. Gao, P. Xi, Q. S. Ren, D. X. Cui, *Mol. Pharm.* **2010**, *7*, 94.
[17] H. Meng, M. Liong, T. Xia, Z. Li, Z. Ji, J. I. Zink, A. E. Nel, *ACS Nano* **2010**, *4*, 4539.